life

Article

Optoacoustic Imaging Offers New Insights into In Vivo Human Skin Vascular Physiology

Luis Monteiro Rodrigues *, Tiago F. Granja and Sergio Faloni de Andrade

CBIOS-Research Centre for Biosciences and Health Technologies, Universidade Lusófona Av, Campo Grande 376, 1749-024 Lisboa, Portugal

* Correspondence: monteiro.rodrigues@ulusofona.pt

Abstract: Functional imaging with new photoacoustic tomography (PAT) offers improved spatial and temporal resolution quality in in vivo human skin vascular assessments. In the present study, we followed a suprasystolic reactive hyperemia (RH) maneuver with a multi-spectral optoacoustic tomography (MSOT) system. A convenience sample of ten participants, both sexes, mean age of 35.8 ± 13.3 years old, was selected. All procedures were in accordance with the principles of good clinical practice and approved by the institutional ethics committee. Images were obtained at baseline (resting), during occlusion, and immediately after pressure release. Observations of the RH by PAT identified superficial and deeper vascular structures parallel to the skin surface as part of the human skin vascular plexus. Furthermore, PAT revealed that the suprasystolic occlusion impacts both plexus differently, practically obliterating the superficial smaller vessels and evoking stasis at the deeper, larger structures in real-time (live) conditions. This dual effect of RH on the skin plexus has not been explored and is not considered in clinical settings. Thus, RH seems to represent much more than the local microvascular reperfusion as typically described, and PAT offers a vast potential for vascular clinical and preclinical research.

Keywords: optoacoustic tomography; PAT; vascular physiology; reactive hyperemia; human upper arm

Citation: Monteiro Rodrigues, L.; Granja, T.F.; de Andrade, S.F. Optoacoustic Imaging Offers New Insights into In Vivo Human Skin Vascular Physiology. *Life* **2022**, *12*, 1628. https://doi.org/10.3390/life12101628

Academic Editors: Marcin Balcerzyk and Riccardo Cicchi

Received: 15 September 2022
Accepted: 14 October 2022
Published: 18 October 2022

1. Introduction

Vascular functional imaging has generated a considerable amount of interest in the last years in preclinical and clinical research. Knowledge of vascular physiology and pathophysiology is critical to the understanding of disease mechanisms [1–4], and recent developments in non-invasive combined sound- and light-based technologies have provided new directions of exploration [1,3–5]. Photoacoustic tomography (PAT) depicts acoustic waves generated by the thermoelastic expansion of structures, typically endogenous chromophores such as hemoglobin and melanin, due to the absorption of light [3,5–8]. This expansion can be quantified, providing real-time information on the circulatory status of the assessed body region.

PAT is regarded as a deep-tissue imaging technology, not comparable to surface imaging techniques such as capillaroscopy and confocal microscopy or to other intermediate imaging techniques such as OCT (optical coherence tomography) [3,8,9]. It is accepted that PAT penetrates deeper with high-resolution than optical tomography and offers better contrast with fewer artifacts than high-resolution sonography [3,5,6,10]. In fact, using ultrasound in place of optical detection eliminates photon scattering. Moreover, considering other comparable technologies, PAT is fast, accurate, and does not use ionizing radiation. For all these reasons, the development of PAT applications has increased in various domains, although with a particular interest in cardiovascular biology. Human skin is often targeted as a primary organ due to its accessibility and the real-time structural, molecular, and metabolic information which may be provided by PAT [3,10–14].

Our research follows these views, assuming that PAT provides a different analytical perspective and a deeper look into these multiple complexities of vascular physiology and pathophysiology [1,2,5,15]. With the (specific) thermoelastic expansion measured, PAT enables a vessel-by-vessel quantification of perfusion-related chromophores, supplying functional information in different (spatial) planes that may allow researchers and physicians to map each circulatory region. By extension, multiple wavelengths of light in multi-spectral optoacoustic tomography (MSOT) enable the separation of different chromophores, reportedly with higher spatial resolution and penetration capacities, and wavelength unmixing and detailed image reconstruction is made with powerful post-acquisition processing [1–5,16].

In the present study, we use an MSOT system to follow the live impact of reactive hyperemia (RH), a classical experimental strategy used to challenge cardiovascular adaptive capacity. Although long used as a predictor of cardiovascular impairment, many questions remain regarding the mechanisms, significance, and applicability of RH responses [17–20]. Here we explore the applicability of the MSOT technology in healthy human vascular physiology by assessing the RH evoked in the flexor forearm by the suprasystolic occlusion of the brachial artery. By the diversity of information provided, we also aim to better understand the adaptive intervenients in RH of the upper limb.

2. Materials and Methods

2.1. MSOT

The MSOT optoacoustic system from iThera Medical GmbH (Munich, Germany) was used. The technical specifications and principles of the system have been detailed elsewhere [5,6,8,16,21–23]. In brief, PAT detects sound waves generated when molecules absorb optical light from a wave laser beam. This evokes a transitory thermoelastic expansion that allows the identification of specific (excited) chromophores, as the signal pattern across the wavelengths measured serves as an exclusive absorption feature for each (chromophore) molecule [5–7].

2.2. Study Population

This exploratory study included ten healthy participants of both sexes, 18 to 60 years old, selected after specific inclusion/non-inclusion criteria and previously informed about the study's purposes and procedures. The primary selection aspects were normotensive, nonsmokers, and free of any chronic disease demanding regular medication or food supplementation. The body mass index (BMI) and mean arterial pressure (MAP) were calculated for all participants (Table 1). Caffeine and alcohol consumption was restricted during the 24 h prior to measurements, as was the application of any topical (including cosmetic) products to the surface of the skin. The study followed the principles of good clinical practice established for human research [24] and was previously approved by the institutional Ethics Committee (Process CE.ECTS/P10.21).

Table 1. General characteristics of selected participants (N = 10).

Participants	Mean ± sd
Sex (F female; M male)	F (5); M (5)
Smokers	0
Physical Activity (h/week)	3.0 ± 1.9
Age, years	35.8 ± 13.3
Body mass, kg	68.2 ± 9.8
Height, m	1.7 ± 0.1
BMI, kg/m^2	23.7 ± 2.5
MAP, mmHg	91.4 ± 4.1

Data tested for normality with D'Agostino and Pearson test in GraphPad Prism with the multi-variable module (Prism version 9 for MacOS); sd—standard deviation.

2.3. Experimental

Before measurements, volunteers were allowed to adapt to the laboratory temperature, humidity, and light (20–30 min).

Circulatory functional imaging was obtained under dynamic conditions through a post-occlusive reactive hyperemia maneuver performed in the upper limb. The pressure cuff was applied in the middle arm while measurements were obtained in the ventral forearm, with the MSOT measurement probe, a 3D cup fixed to the surface of the forearm by a flexible metal arm [16]. After baseline scan acquisition, the cuff was rapidly inflated with 200 mmHg to occlude the brachial artery. This pressure was maintained for one minute to ensure hemodynamical stabilization in the area. The cuff was then rapidly deflated, and videos were recorded during the immediate post-occlusion recovery. Throughout the experimental procedure, the main chromophores oxyhemoglobin HbO_2 and deoxyhemoglobin Hb were simultaneously visualized (in real-time) by the MSOT system.

Videos were post-processed for image reconstruction by the ViewMSOT software (iThera Medical version 4.0). MSOT software was used to collect data from selected regions of interest (ROI) and to quantify HbO_2, Hb, HbT (total hemoglobin, the sum of HbO_2 and Hb), and the mean saturation of oxygen ($mSO_{2)}$ during the different stages of the experiments. Image J software (National Institutes of Health, version 1.53k14) was also used in the image reconstruction process.

2.4. Statistical Analysis

Statistical analysis was performed in GraphPad Prism 9.2.0.283 MachineID: 0861F12-DB8D10. Normal distribution was tested with the Kolmogorov–Smirnov test and direct observation of generated QQ plots.

3. Results and Discussion

MSOT scans provided images in frontal, transversal, and longitudinal planes, from which various ROIs might be selected for further calculations. Baseline scans obtained in the (central) flexor forearm were compared with the occlusion and post-occlusion scans in the same area. High-resolution images were assessed at different depths detailing the skin microcirculation organization at this site. PAT consistently revealed two vascular plexuses parallel to the skin surface—larger vessels located 2 to 6 mm below the skin surface corresponding to the deep plexus and smaller vessels located 0.6 to 2 mm below the skin. The capillary structures corresponding to the papillary dermis were difficult to visualize (Figure 1). Perpendicular structures connecting both plexus and deeper vascular structures, likely crossing subcutaneous tissue and/or muscle, were also visible (Figure 1). Considering this resolution capacity, the aim of our study was to visualize and quantify the impact of a real-time RH procedure in both plexuses.

Through the ROI analysis of the MSOT scan images, $HbO_{2,}$ Hb, HbT, and mSO_2 can be determined [16,21,22]. HbT and SO_2 are semi-quantitative physiological parameters automatically calculated for each pixel whenever both Hb and HbO_2 components are unmixed. According to the instrument manufacturer, different fluence and spectral coloring will consistently impair the comparison of these MSOT descriptors with similar from other technologies. Thus, 'm' is used to designate MSOT-derived oxygen saturation [22]. HbT refers to the semi-quantitative sum of unmixed deoxy- and oxy-hemoglobin components calculated from all pixels after setting negative pixels in Hb and HbO_2 to 0 [22]. mSO_2 represents the MSOT-derived fraction of oxygenated hemoglobin divided by total hemoglobin, where mSO_2 is calculated if (and only if) a pixel has Hb > 0 and HbO_2 > 0 [22].

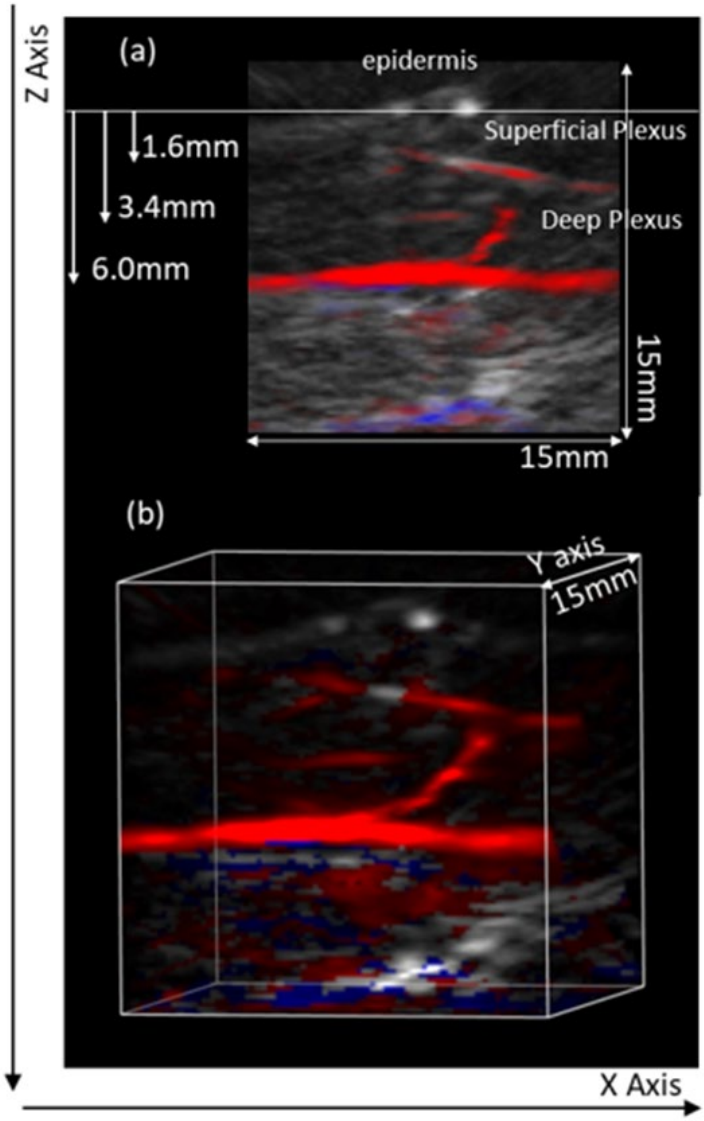

Figure 1. Illustrative images from the flexor aspect of the human forearm obtained with the MSOT technology. (**a**) Different vascular structures parallel to the skin surface are seen at different depths and assumed to correspond to the superficial and the deep skin plexuses; the different diameters seen are consistent with this assumption. The vascular structure running perpendicular likely corresponds to an arteriole connecting both plexuses. Some deeper structures might also be present in the same ROI. (**b**) The same structures shown in a 3D view.

Image reconstruction focused on our chromophores of interest (Figure 2) indicates that the suprasystolic pressure clearly decreases HbO_2 in the superficial plexus due to the collapse of those vessels, while HbO_2 seems to increase at the deeper skin plexus, likely due to some transfer of blood from higher structures but also due to stasis and reduction of the capacity of (O_2) transfer to the tissues. Following the pressure release, the HbO_2 signal slowly increased at the surface and decreased in the lower skin plexus. During the experiments, Hb concentration profiles consistently evolved in the opposite direction in both plexus (Figure 3). The calculated mSO_2 decreased in both plexuses with occlusion, with slow recovery (increase) after cuff deflation (Figure 4).

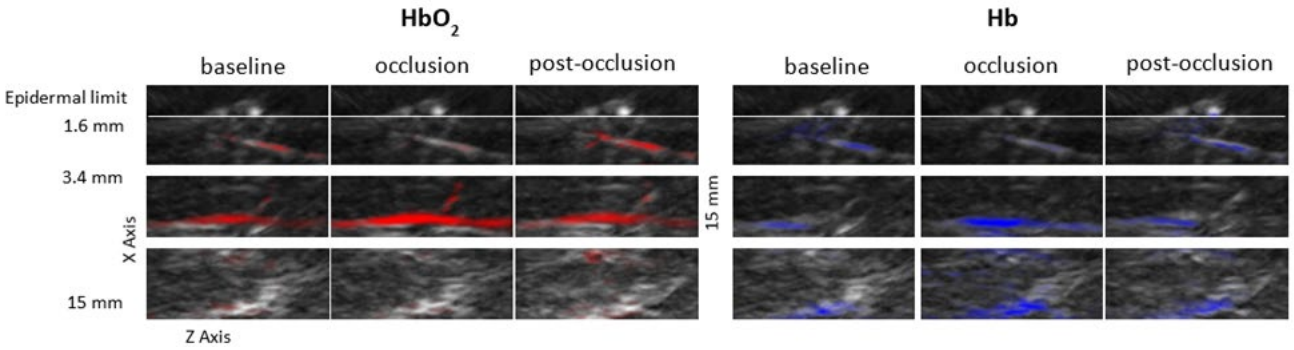

Figure 2. Illustrative images of HbO_2 (**red**) and Hb (**blue**) from the flexor aspect of the human forearm obtained with the MSOT technology during the reactive hyperemia induced by arterial occlusion with suprasystolic pressure. Different vascular structures parallel to the skin surface are depicted by the different colored chromophores at different depths during the different phases of the experimental protocol and are assumed to correspond to the superficial and the deep skin plexus. Additional subcutaneous structures can also be detected at deeper locations, although with reduced resolution.

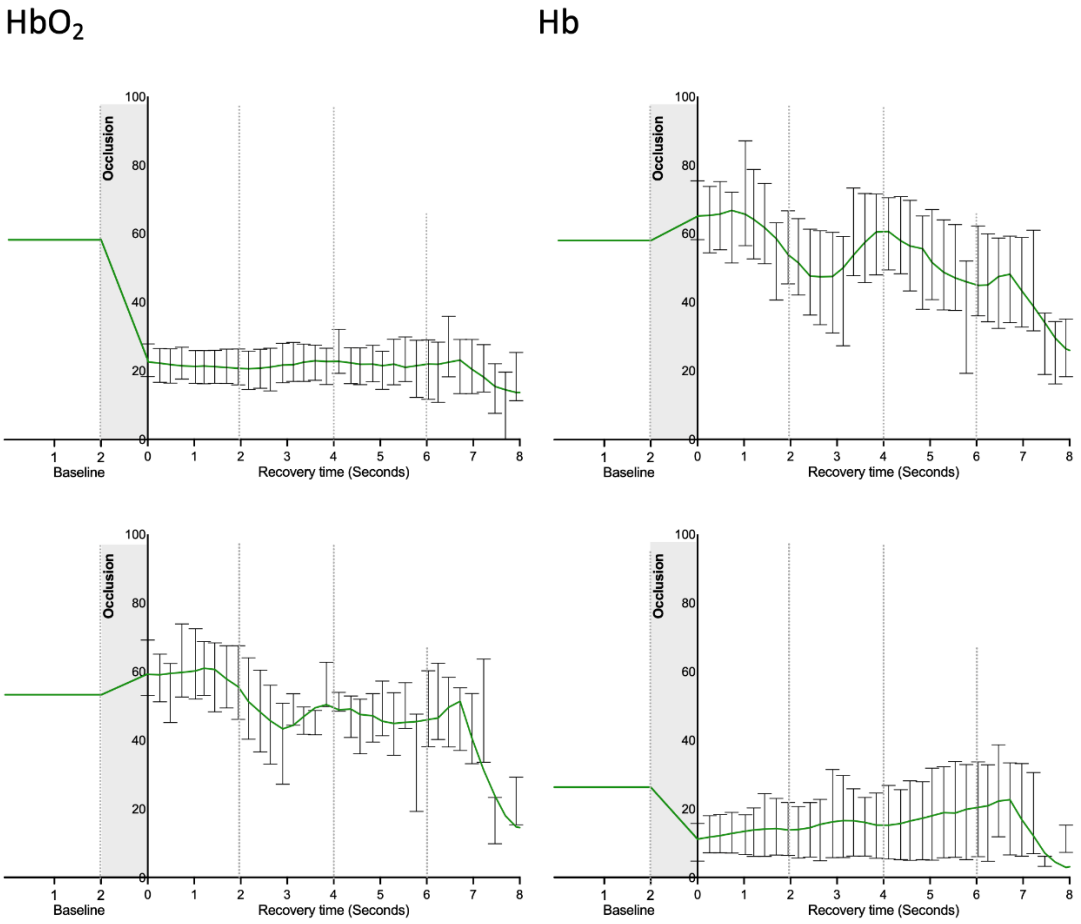

Figure 3. HbO_2 and Hb signals obtained in the superficial (**top**) and the deeper skin plexus (**bottom**) of healthy participants (n = 10) during the experimental RH protocol. As shown, these parameters progress in different directions during the procedure, indicating that the suprasystolic occlusion has different effects at different depths, affecting global hemodynamics (please see text). Signals are quantified by MSOT based on the identification of the respective chromophores (values correspond to mean and SEM; data distribution was tested with the Kolmogorov–Smirnov test.

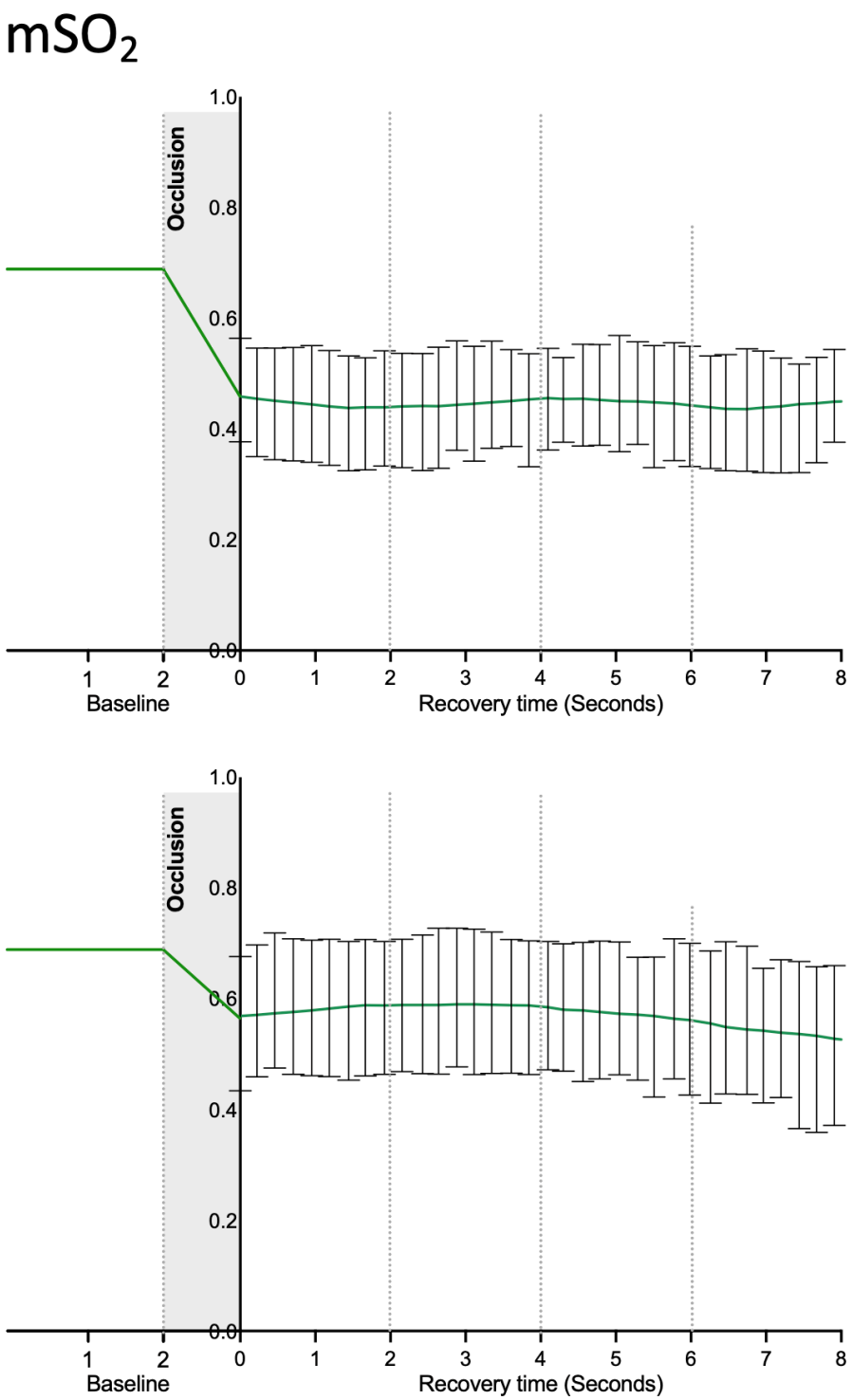

Figure 4. MSOT-derived oxygen saturation (mSO_2) signals obtained in the superficial (**top**) and the deeper skin plexus (**bottom**) of healthy participants (n = 10) during the experimental RH protocol (please see text). Signals are quantified by MSOT based on the identification of the respective chromophores (values correspond to mean and SEM; data distribution was tested with the Kolmogorov–Smirnov test).

RH is a widely used functional challenger used in vascular research. Mechanisms of this response to ischemia in the human skin microcirculation are not clearly understood. Still, RH is accepted to represent the magnitude of reperfusion in that anatomical location following a (short) period of arterial occlusion [17–20]. Both metabolic and myogenic

components seem to be present, but past studies suggest that sensory nerves play a central role [3,17,25].

A principal concern involves the distinction between venous and arterial occlusion. Measurements are normally performed after occluding macrocirculation vessels (the brachial artery in the arm, as an example) to assess microcirculation through the skin. It is known that venous and arterial systems interact permanently to adjust local and systemic hemodynamics. Therefore, the perfusion changes caused by RH are certainly influenced by venous dynamics during the occlusion–disocclusion process [26,27]. Even so, weak RH reperfusion is commonly regarded as a sign of (micro)vascular impairment [17,19,20].

These questions, partially explained by time-related technological limitations, motivated RH exploration with other instruments in addition to plethysmography and laser Doppler flowmetry. RH has been investigated with near-infrared spectroscopy (NIRS) [28,29] and compared with PAT [30], assessed with diffuse correlation spectroscopy (DCS) [31], contrast-enhanced ultrasound (CEUS) [32], and peripheral artery tonometry [33]. Although these studies confirm the possibility of the use of quantifiable metabolic and molecular variables, together with image(s), in clinical and preclinical settings, there is still no agreement about outcomes. Stronger correlations for the "time-to-peak" variable from CEUS and NIRS were recently reported [32]. Moreover, the venous and arterial involvement in RH is still not properly controlled in typical procedures, meaning that the vascular responsiveness of both micro and macrocirculation at different depths cannot be clearly distinguished [17,28,29,34,35]. Additionally, recent data from DCS suggests that skin circulation is not the best model to study skeletal muscle vasculature by RH [31].

In our study, we demonstrate for the first time, to the best of our knowledge, the in vivo functioning of skin plexus under suprasystolic pressure. While the smaller vessels of the superficial plexus immediately collapse when pressure rises and perfusion is nearly reduced to zero, the opposite effect is observed at the deep plexus, where larger vessels and higher amounts of blood are present with blood accumulating on site, enlarging these structures and increasing their visibility (Figure 2). The main chromophores HbO_2 and Hb, along with calculated mSO_2, progress accordingly (Figures 3 and 4). We believe from the present data that the deeper vascular structures shown correspond to the deeper skin plexus and not to the muscle beneath.

It is also clear that the intensity and duration of the occlusion clearly affect the procedure. The separate control of venous and arterial occlusion by using different cuff pressures offers multiple controversies [27,28,30,36]. We opted for the application of 200 mmHg suprasystolic pressure in our study to ensure arterial occlusion, confident that pressure affects multiple structures in depth and involves more than the microcirculatory units in the area. This is in line with previous findings showing that the RH response to the arterial occlusion of one limb was detectable in the contra-lateral non-occluded limb [32,37,38]. This observation suggests that RH involves a centrally mediated control we previously termed as a prompt adaptive hemodynamical response (PAHR) [39].

In the present study conditions, the use of PAT to monitor RH not only fills the gap between morphology and function but also suggests that RH represents much more than the previously believed local microvascular reperfusion. Further, the microcirculatory detail provided with these results indicates that the predictive value of RH in clinical practice still faces important challenges.

Our study should be regarded as exploratory, as our focus was limited and our population small. Nevertheless, it is clear that PAT technologies have great advancement potential for functional vascular imaging, with remarkable clinical potential.

Author Contributions: Conceptualization, L.M.R.; Data curation, T.F.G.; Investigation, S.F.d.A.; Methodology, L.M.R. and T.F.G.; Supervision, L.M.R.; Validation, L.M.R.; Writing—original draft, L.M.R., T.F.G. and S.F.d.A.; Writing—review & editing, L.M.R. All authors have read and agreed to the published version of the manuscript.

Funding: This research is funded by ALIES and COFAC, the principal providers of the technology under study, and by Fundação para a Ciência e a Tecnologia (FCT) through the grant UIDB/04567/2020 to CBIOS.

Institutional Review Board Statement: As stated above, the study was conducted in accordance with the Declaration of Helsinki, and approved by the School of Health Ethics Committee (Process CE.ECTS/P10.21) for studies involving humans.

Conflicts of Interest: All authors have stated that there are no financial and/or personal relationships that could represent a potential conflict of interest.

References

1. Guven, G.; Hilty, M.P.; Ince, C. Microcirculation: Physiology, Pathophysiology, and Clinical Application. *Blood Purif.* **2020**, *49*, 143–150. [CrossRef] [PubMed]
2. Gopcevic, K.R.; Gkaliagkousi, E.; Nemcsik, J.; Acet, Ö.; Bernal-Lopez, M.R.; Bruno, R.M.; Climie, R.E.; Fountoulakis, N.; Fraenkel, E.; Fraenkel, A.; et al. Pathophysiology of Circulating Biomarkers and Relationship With Vascular Aging: A Review of the Literature From VascAgeNet Group on Circulating Biomarkers, European Cooperation in Science and Technology Action 18216. *Front. Physiol.* **2021**, *12*, 789690. [CrossRef] [PubMed]
3. Cracowski, J.L.; Roustit, M. Human Skin Microcirculation. *Compr. Physiol.* **2020**, *10*, 1105–1154. [CrossRef] [PubMed]
4. Tiwari, A.; Elgrably, B.; Saar, G.; Vandoorne, K. Multi-Scale Imaging of Vascular Pathologies in Cardiovascular Disease. *Front. Med.* **2022**, *8*, 754369. [CrossRef]
5. Li, D.; Humayun, L.; Vienneau, E.; Vu, T.; Yao, J. Seeing through the Skin: Photoacoustic Tomography of Skin Vasculature and Beyond. *JID Innov.* **2021**, *1*, 100039. [CrossRef]
6. Hu, S.; Wang, L.V. Photoacoustic imaging and characterization of the microvasculature. *J. Biomed. Opt.* **2010**, *15*, 011101. [CrossRef]
7. Wang, L.V. Prospects of photoacoustic tomography. *Med. Phys.* **2008**, *35*, 5758–5767. [CrossRef]
8. Xia, J.; Yao, J.; Wang, L.V. Photoacoustic tomography: Principles and advances. *Electromagn. Waves* **2014**, *147*, 1–22. [CrossRef]
9. Lal, C.; Leahy, M.J. An Updated Review of Methods and Advancements in Microvascular Blood Flow Imaging. *Microcirculation* **2016**, *23*, 345–363. [CrossRef]
10. Taruttis, A.; Herzog, E.; Razansky, D.; Ntziachristos, V. Real-time imaging of cardiovascular dynamics and circulating gold nanorods with multispectral optoacoustic tomography. *Opt. Express* **2010**, *18*, 19592–19602. [CrossRef]
11. Wang, H.; Shan, Z.; Li, W.; Chu, M.; Yang, J.; Yi, D.; Zhan, J.; Yuan, Z.Y.; Raikwar, S.; Wang, S.; et al. Guidelines for assessing mouse endothelial function via ultrasound imaging: A report from the International Society of Cardiovascular Translational Research. *J. Cardiovasc. Transl. Res.* **2015**, *8*, 89. [CrossRef] [PubMed]
12. Zafar, H.; Breathnach, A.; Subhash, H.M.; Leahy, M.J. Linear-array-based photoacoustic imaging of human microcirculation with a range of high frequency transducer probes. *J. Biomed. Opt.* **2015**, *20*, 51021. [CrossRef] [PubMed]
13. Chen, Z.; Rank, E.; Meiburger, K.M.; Sinz, C.; Hodul, A.; Zhang, E.; Hoover, E.; Minneman, M.; Ensher, J.; Beard, P.C.; et al. Non-invasive multimodal optical coherence and photoacoustic tomography for human skin imaging. *Sci. Rep.* **2017**, *7*, 17975. [CrossRef] [PubMed]
14. Xu, D.; Yang, S.; Wang, Y.; Gu, Y.; Xing, D. Noninvasive and high-resolving photoacoustic dermoscopy of human skin. *Biomed. Opt. Express* **2016**, *7*, 2095–2102. [CrossRef] [PubMed]
15. Bruno, R.M.; Climie, R.; Gallo, A. Aortic pulsatility drives microvascular organ damage in essential hypertension: New evidence from choroidal thickness assessment. *J. Clin. Hypertens.* **2021**, *23*, 1039–1040. [CrossRef] [PubMed]
16. Granja, T.; de Andrade, S.F.; Rodrigues, L.M. Multispectral Optoacoustic Tomography for Functional Imaging in Vascular Research. *J. Vis. Exp.* **2022**, *184*, e63883. [CrossRef]
17. Rosenberry, R.; Nelson, M.D. Reactive hyperemia: A review of methods, mechanisms, and considerations. American journal of physiology. *Regul. Integr. Comp. Physiol.* **2020**, *318*, R605–R618. [CrossRef]
18. Ishibashi, Y.; Takahashi, N.; Shimada, T.; Sugamori, T.; Sakane, T.; Umeno, T.; Hirano, Y.; Oyake, N.; Murakami, Y. Short duration of reactive hyperemia in the forearm of subjects with multiple cardiovascular risk factors. *Circ. J.* **2006**, *70*, 115–123. [CrossRef]
19. Huang, A.L.; Silver, A.E.; Shvenke, E.; Schopfer, D.W.; Jahangir, E.; Titas, M.A.; Shpilman, A.; Menzoian, J.O.; Watkins, M.T.; Raffetto, J.D.; et al. Predictive value of reactive hyperemia for cardiovascular events in patients with peripheral arterial disease undergoing vascular surgery. *Arter. Thromb. Vasc Biol.* **2007**, *27*, 2113–2119. [CrossRef]
20. Paine, N.J.; Hinderliter, A.L.; Blumenthal, J.A.; Adams, K.F., Jr.; Sueta, C.A.; Chang, P.P.; O'Connor, C.M.; Sherwood, A. Reactive hyperemia is associated with adverse clinical outcomes in heart failure. *Am. Heart J.* **2016**, *178*, 108–114. [CrossRef]
21. Granja, T.; Andrade, S.; Rodrigues, L. Optoaccoustic Tomography—good news for microcirculatory research Biomedical and Biopharmaceutical Research. *PAT* **2021**, *18*, 200–212. [CrossRef]
22. iThera Scientific Instruction Manual—MSOT Invasion. User's Guide 2021. Available online: https://www.usf.edu/research-innovation/comparative-medicine/documents/training/msot-invision-series-user-manual-3-user-guide.pdf (accessed on 10 October 2022).

23. Yang, F.F.; Cao, L.; Wen, H.; Fu, T.T.; Ma, S.Q.; Liu, C.Y.; Quan, L.H.; Liao, Y.H. Multispectral optoacoustic tomography (MSOT) for imaging the particle size-dependent intratumoral distribution of polymeric micelles. *Int. J. Nanomed.* **2018**, *13*, 8549–8560. [CrossRef]
24. World Medical Association. World Medical Association Declaration of Helsinki: Ethical principles for medical research involving human subjects. *JAMA* **2013**, *310*, 2191–2194. [CrossRef] [PubMed]
25. Lorenzo, S.; Minson, C.T. Human cutaneous reactive hyperaemia: Role of BKCa channels and sensory nerves. *J. Physiol.* **2007**, *585 Pt 1*, 295–303. [CrossRef]
26. Alomari, M.A.; Solomito, A.; Reyes, R.; Khalil, S.M.; Wood, R.H.; Welsch, M.A. Measurements of vascular function using strain-gauge plethysmography: Technical considerations, standardization, and physiological findings. *Am. J. Physiol. Heart Circ. Physiol.* **2004**, *286*, H99–H107. [CrossRef]
27. Bahadir, Z.; Tisdell, E.; Arce Esquivel, A.A.; Dobrosielski, D.A.; Welsch, M.A. Influence of venous emptying on the reactive hyperemic blood flow response. *Dyn. Med.* **2007**, *6*, 3. [CrossRef]
28. Dennis, J.J.; Wiggins, C.C.; Smith, J.R.; Isautier, J.M.; Johnson, B.D.; Joyner, M.J.; Cross, T.J. Measurement of muscle blood flow and O_2 uptake via near-infrared spectroscopy using a novel occlusion protocol. *Sci. Rep.* **2021**, *11*, 918. [CrossRef]
29. McLay, K.M.; Nederveen, J.P.; Pogliaghi, S.; Paterson, D.H.; Murias, J.M. Repeatability of vascular responsiveness measures derived from nearinfrared spectroscopy. *Physiol. Rep.* **2016**, *4*, e12772. [CrossRef]
30. Yang, J.; Zhang, G.; Chang, W.; Chi, Z.; Shang, Q.; Wu, M.; Pan, T.; Huang, L.; Jiang, H. Photoacoustic imaging of hemodynamic changes in forearm skeletal muscle during cuff occlusion. *Biomed. Opt. Express* **2020**, *11*, 4560–4570. [CrossRef]
31. Didier, K.D.; Hammer, S.M.; Alexander, A.M.; Caldwell, J.T.; Sutterfield, S.L.; Smith, J.R.; Ade, C.J.; Barstow, T.J. Microvascular blood flow during vascular occlusion tests assessed by diffuse correlation spectroscopy. *Exp. Physiol.* **2020**, *105*, 201–210. [CrossRef]
32. Young, G.M.; Krastins, D.; Chang, D.; Lam, J.; Quah, J.; Stanton, T.; Russell, F.; Greaves, K.; Kriel, Y.; Askew, C.D.; et al. Influence of cuff-occlusion duration on contrast-enhanced ultrasound assessments of calf muscle microvascular blood flow responsiveness in older adults. *Exp. Physiol.* **2020**, *105*, 2238–2245. [CrossRef] [PubMed]
33. Young, G.M.; Krastins, D.; Chang, D.; Lam, J.; Quah, J.; Stanton, T.; Russell, F.; Greaves, K.; Kriel, Y.; Askew, C.D. The Association Between Contrast-Enhanced Ultrasound and Near-Infrared Spectroscopy-Derived Measures of Calf Muscle Microvascular Responsiveness in Older Adults Heart. *Lung Circ.* **2021**, *30*, 1726–1733. [CrossRef] [PubMed]
34. Matsuzawa, Y.; Kwon, T.G.; Lennon, R.J.; Lerman, L.O.; Lerman, A. Prognostic value of flow-mediated vasodilation in brachial artery and fingertip artery for cardiovascular events: A systematic review and metaanalysis. *J. Am. Heart Assoc.* **2015**, *4*, e002270. [CrossRef]
35. Braverman, I.M. The Cutaneous Microcirculation. *J. Investig. Dermatol. Symp. Proc.* **2000**, *5*, 3–9. [CrossRef]
36. Karlas, A.; Kallmayer, M.; Fasoula, N.-A.; Liapis, E.; Bariotakis, M.; Krönke, M.; Anastasopoulou, M.; Reber, J.; Eckstein, H.H.; Ntziachristos, V. Multispectral optoacoustic tomography of muscle perfusion and oxygenation under arterial and venous occlusion: A human pilot study. *J. Biophotonics* **2020**, *13*, e201960169. [CrossRef] [PubMed]
37. Rodrigues, L.M.; Rocha, C.; Ferreira, H.A.; Silva, H.N. Lower limb massage in humans increases local perfusion and impacts systemic hemodynamics. *J. Appl. Physiol.* **2020**, *128*, 1217–1226. [CrossRef] [PubMed]
38. Rodrigues, L.M.; Silva, H.; Ferreira, H.; Renault, M.A.; Gadeau, A.P. Observations on the perfusion recovery of regenerative angiogenesis in an ischemic limb model under hyperoxia. *Physiol. Rep.* **2018**, *6*, e13736. [CrossRef]
39. Florindo, M.; Nuno, S.; Andrade, S.; Rocha, C.; Rodrigues, L.M. The Acute Modification of the Upper-Limb Perfusion in Vivo Evokes a Prompt Adaptive Hemodynamic Response to Re-Establish Cardiovascular Homeostasis. Physiology21 Annual Conference Abstract Book 2021. Available online: https://static.physoc.org/app/uploads/2021/06/10115155/Physiology-2021-Abstract-Book.pdf (accessed on 10 October 2022).